Journal of the Australian Ceramic Society
https://doi.org/10.1007/s41779-025-01191-2

RESEARCH

Core–shell powder strategy for additive manufacturing of ceramics: application to direct powder bed selective laser processing of silicon carbide

Alejandro Montón[1,2] · Francis Maury[1] · Geoffroy Chevallier[3] · Claude Estournès[3] · Marc Ferrato[4] · David Grossin[1]

Received: 11 May 2023 / Revised: 17 February 2025 / Accepted: 25 March 2025

Abstract
The production of innovative ceramic powders through surface functionalization of grains, featuring a core–shell structure, accelerates mass diffusion and enhances sintering behavior. This approach significantly impacts the additive manufacturing field. In this study, a commercial SiC preceramic compound from the polycarbosilane family, specifically poly(silaethylene), was grafted onto the surface of Silicon Carbide (SiC) particles, forming a conformal molecular layer. Powder Bed Selective Laser Processing, also known as Selective Laser Sintering/Melting, was employed to fabricate 3D SiC and surface-modified SiC parts, enabling a comparative analysis of the efficiency and impact of surface modification in the manufacturing process. The surface functionalization increases densification by at least 5% without affecting the final phases of the manufactured parts. Additionally, Spark Plasma Sintering (SPS) was employe as a post-treatment to further densify the samples, increasing their final density and eliminating residual silicon and carbon, which are produced due to the undesired decomposition of SiC during the manufacturing process.

Keywords Silicon carbide · Powder bed fusion · Selective laser sintering · Powder surface modification · Polymer derived ceramic · Core–shell structure

Introduction

Silicon Silicon Carbide (SiC) is a ceramic material with excellent properties such as high mechanical stiffness, low density, wide bandgap, low coefficient of expansion, high thermal stability, and resistance to corrosive environments [1]. Due to its unique properties, SiC is widely used in many fields, such as automotive [2], electronics [3], aerospace [4, 5], and the military industry.

In recent years, additive manufacturing (AM) has been extensively studied due to the enormous advantages of manufacturing complex structural ceramics. One additive manufacturing method, Powder Bed Selective Laser Processing (PBSLP) [6], also called Laser Powder Bed Fusion (L-PBF) [7], or Selective Laser Sintering/Melting (SLS/SLM), has shown promise in fabricating complex SiC components. However, this process is particularly challenging since SiC does not have a melt phase under normal atmospheric conditions but instead decomposes at temperatures around 2545 °C into liquid Si and solid C [8]. Consequently, melting of SiC does not occur. Moreover, pressureless sintering of refractory materials like SiC, without additives, is also difficult [9]. For these reasons, indirect PBSLP is generally used to form SiC ceramic components by sintering/melting polymer binders in a composite powder. However, indirect methods require debinding and post-sintering processes, which can lead to shrinkage and defects.

In some recent experimental works on manufacturing SiC using indirect PBSLP, Jin et al. combined selective laser sintering (SLS), cold isostatic pressing (CIP), and polymer infiltration pyrolysis (PIP) to manufacture

✉ Alejandro Montón
alejandromonton@unizar.es

1 CIRIMAT, Université de Toulouse, CNRS, INP- ENSIACET 4 Allée Émile Monso, 31432 Toulouse Cedex 4, France

2 Defense University Centre Zaragoza: Centro Universitario de La Defensa, Zaragoza, Spain

3 CIRIMAT, Université de Toulouse, CNRS, Université Toulouse 3 - Paul Sabatier, 118 Route de Narbonne, 31062 Toulouse Cedex 9, France

4 MERSEN Boostec, ZAECeram'InnovPyrénées, 65460 Bazet, France

Published online: 08 April 2025

complex SiC parts. The powder used for SLS was a mixture of SiC powder and epoxy resin (3 wt%). However, during degreasing, some carbon remained in the specimen due to resin carbonization. This work also mentioned the use of polycarbosilane for polymer infiltration pyrolysis for the first time in additive manufacturing processes [10]. Liu et al. combined selective laser sintering (PBSLP), CIP, and reaction sintering (RS). In this process, a Phenol formaldehyde resin (PF)-SiC composite powder was prepared using mechanical mixing and cold coating methods, with an optimized PF content of 18 wt%. To improve the density of the sintered body after final reaction sintering, carbon black was added to the initial mixed powder. The final sintered SiC bodies achieved a bending strength of 292–348 MPa and a density of 2.94–2.98 g/cm3 using the PF-coated SiC-C composite powder and the LS/CIP/RS process [11]. Song et al. combined the reaction-bonded (RB) process with selective laser sintering (PBSLP) to improve the performance of SiC/Si composites. They studied the effects of an epoxy resin binder on the performance and microstructure of preforms and sintered bodies. Based on the results, graphite with low reactivity was used as a slow-release carbon source to promote sintering densification and improve the carbon density of preforms [12].

For direct PBSLP of SiC or Reaction Bonded SiC, typically, an initial powder mixture of SiC and silicon (Si) powders is used because Si melts and re-solidifies to bind the primary SiC particles. These Si-SiC preforms are then impregnated with a phenolic resin, which is pyrolyzed to yield porous carbon. This carbon undergoes a secondary reaction, forming SiC when the preforms are infiltrated with molten silicon in the final step, resulting in reaction-bonded SiC parts (RBSiC). However, achieving fully dense RBSiC sacrifices the optimization of mechanical properties compared to pure SiC, and residual Si limits its use in chemical applications. Meyers et al. demonstrated this process, achieving fully dense RBSiC parts with up to 84 vol% SiC. The optimized Si-SiC exhibited a Vickers hardness of 2045 HV, an electrical conductivity of 5.3 × 103 S/m, a Young's modulus of 285 GPa, and a four-point bending strength of 162 MPa [13]. Montón et al. manufactured SiC parts using direct PBSLP without post-treatments or additives in the initial powder mixture. The optimization of process parameters was performed through numerical and experimental analysis. The optimal parameters were set at laser power: 45 W, scanning speed: 250 mm/s, layer thickness: 30 µm, hatching distance: 35 µm, scanning strategy: hexagonal rotated by 90 degrees between layers, and compaction: 100%. The final SiC parts exhibited 81% relative density and 5 wt% and 1 wt% residual silicon and carbon, respectively, due to decomposition during the process from high temperature peaks generated by the scanning strategy [14, 15]. Moreover, the process viability was confirmed by manufacturing complex SiC shapes, such as SiC lattice structures, which cannot be achieved with traditional manufacturing techniques.

In the present study extends and complete our current research program on direct PBSLP of SiC [14] by using an innovative ceramic powder, consisting of surface modified SiC grains featuring a core-shell architecture. Density, porosity distribution, microstructure and chemical analysis were investigated. Moreover, Spark Plasma Sintering (SPS), an advanced process that is also used to consolidate silicon carbide powder without additives [16, 17], has been used in order to improve the structural homogeneity and mechanical properties of the parts. Recently, Levy et al. [14] reported significant improvement in the final manufactured part properties by applying uniaxial pressure within SPS apparatus in laminated carbon steel structures. Eqtesadi et al. combined robocasting and pressureless spark plasma sintering for the first time to fabricate geometrically complex B4 C components [18]. Manière [19] et al. proved the ability of SPS technology to perform the total densification of highly complex shape samples with an approach they called the "deformed interfaces method" that uses sacrificial materials. This method was tested with different materials (Al, CoNiCrAlY, PMMA, Al_2O_3, 4Y-ZrO_2) and high complex shapes. Therefore, SPS offers a versatile solution as post-treatment of complex additive manufactured parts, where other post-treatments techniques, such as cold isostatic pressing, still limits the use of some specific complex shapes or structures. Figure 1 shows the general schematic research process followed by this research work.

The original scientific approach of this work lies in the production of innovative ceramic powders, featuring a core-shell structure, for application in additive manufacturing. This method has a profound technological impact on the additive manufacturing field. As schematically described in Fig. 2, various surface modification methods and combinations can reduce sintering temperatures or enhance specific material properties in AM of ceramics. For instance, using some coated pressureless sintering additives in the form of polymer-derived ceramics, such as polycarbosilane, can yield SiC and enhance the sintering of Al_2O_3 [20]. Another example is the use of grafted additives with low melting points to promote liquid phase sintering and reduce sintering temperatures in ceramics. A similar concept has been applied to metallic powders by using Cu-coated Ni-alloy powder and Cu-coated Fe powders [21]. In the case of two-component powders, melting one of the coated components with the lower melting point forms the liquid phase. Additionally, viscosity and absorptance coated modifiers could also be used, among other possibilities.

Specifically, in this work, by using this core–shell structure method, SiC powders that enable with functionalized grain surface have been produced for their applications in direct PBSLP. This surface modification, where a SiC preceramic

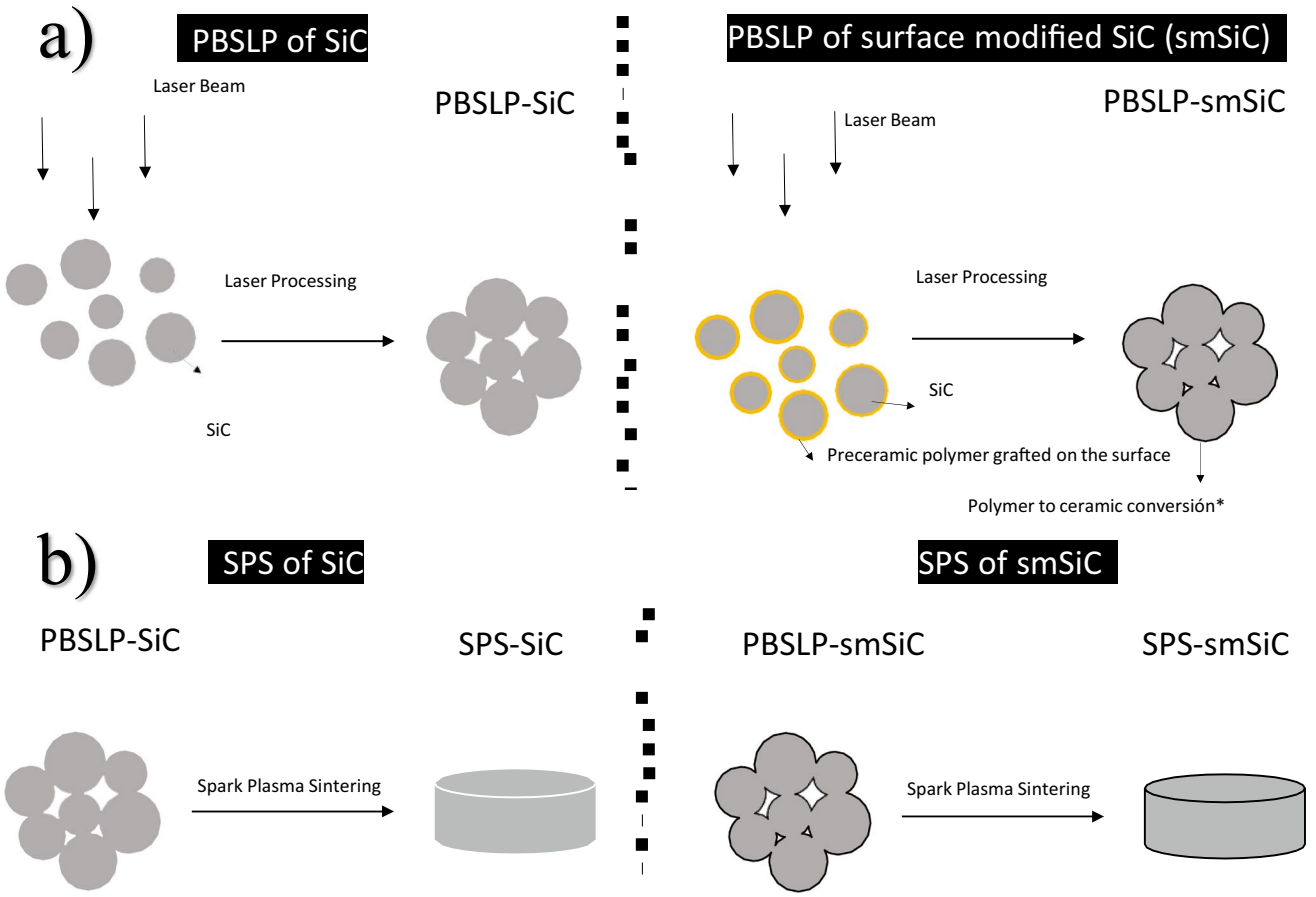

Fig. 1 Description of the combined process (**a**) PBSLP, **b**) SPS) starting with either SiC powder or surface modified smSiC powder to manufacture dense SiC parts. *Preceramic polymer is converted into silicon carbide as an integral part of the final material structure

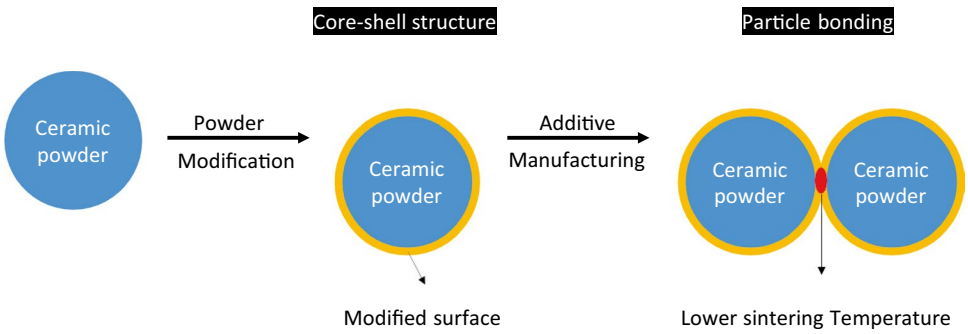

Fig. 2 Use of surface powder modification as core–shell structure to promote sintering

precursor is grafted onto the grain surface of SiC powder, is a method to enhance the sintering behaviour of this ceramic material. As we demonstrated in a previous work [22], dense SiC and surface modified SiC (smSiC) specimens were directly fabricated by SPS process at 2200 °C and 50 MPa for only 1 min in this steady stage. The SiC specimens achieved a density of 2.929 ± 0.007 g•cm^{-3} (91% relative density), while the smSiC samples reached a density of 3.048 ± 0.046 g•cm^{-3} (96% relative density) under identical SPS conditions. Notably, the densification process consistently exhibited superior results for smSiC compared to the raw SiC samples.

Materials and methods

For this study, Alpha-SiC (α-SiC; d50 = 20 µm; Mersen Boostec) was utilized. The particle size distribution was determined using the Mastersizer 3000 (Malvern

Panalytical) laser diffraction particle size analyzer. Despite the powder's irregular shape, which could potentially lead to challenges in layer deposition due to increased inter-particle friction, it was successfully deposited layer by layer on the 3D printer bed without any defects or issues. This is noteworthy since powders commonly used in laser sintering are typically spherical or have rounded edges.

In this work, a commercial compound from the polycarbosilane family, specifically poly(silaethylene) (PSE) supplied by Starfire® System (CVD- 4000), was used for the surface functionalization of silicon carbide powder. This preceramic precursor is a SiC-forming polymer known to produce stoichiometric silicon carbide coatings (Si:C = 1:1) without the need for additional reactants via chemical vapor deposition [18]. The grafting process creates a conformal coverage of a molecular layer onto the surface of SiC particles, avoiding the excess oligomer that can be provided by the feed powder.

PSE has been grafted onto the surface of SiC particles in the form of a conformal coverage molecular layer following the protocols reported in the literature [22]. It is crucial in the grafting process to avoid attaching an excessive amount of polymer to the powder surface. This precaution is essential to prevent an undesired increase in specific surface area, significant alterations in powder morphology, and difficulties in infiltrating the coupling agent into the particle agglomerates. Excessive polymer presence could compromise graft efficiency, negatively impact powder flowability, and render it unsuitable for the PBSLP process.

The flowability of both SiC and surface-modified SiC (smSiC) was assessed using the dynamic angle of repose. This characterization technique is widely accepted for measuring powder flowability and is recommended by ASTM for characterizing metal powders for additive manufacturing (AM) [23]. The angle was measured using Hosokawa Micron's Powder Characteristics Tester PT-S. The average angle of repose obtained from this test was 41 ± 3° and 44 ± 2° for the SiC powder and smSiC respectively, which can be considered an adequate value for the AM process [24].

The PBSLP experiment was conducted on a Phenix™ Systems ProX® DMP 200 3D printer manufactured by 3D Systems and equipped with Fiber laser of 300 W maximum power (laser wavelength = 1060 nm, spot size = 70 µm). Laser Power (P) in the range of 35–55 W, scanning speed (v) in the range of 50–1000 mm/s, layer thickness in the range of 20–40 µm, hatching distance in the range of 17.5–100 µm and powder cylinder compaction in the range of 0–100% were used (Table 1). The scanning strategy was following a hexagonal pattern rotated by 90 degrees between layers, as recommended from our last study [25]. The manufactured parts had a dimension of 10x10x10 mm^3. PBSLP was conducted in an inert argon atmosphere to prevent the oxidation during the process.

The SiC 3D components underwent spark plasma sintering using a Dr. Sinter 2080 unit from SPS Syntex Inc., Japan, located at the Plateforme Nationale CNRS de Frittage Flash within the Université Toulouse 3 Paul Sabatier in France. The SiC 3D parts were placed into graphite dies. Before this step, a graphite foil (PERMA-FOIL®Toyo Tanso) was consistently applied to cover the inside wall of the die, as well as the interfaces between the punches/sample and spacers/electrodes. To minimize heat loss during the experiment, the outside wall of the die was consistently covered with a graphite felt. Additionally, graphite powder was introduced to fill the vacant space between the graphite dies and the sample. A heating rate of 300 °C/min was used from room temperature to 600 °C, where a 1 min dwelling time was applied. Then, a heating rate of 100 °C/min between 600 and 2200 °C was applied. An optical pyrometer (IR-AH series Chino), focused inside a little hole (1.8 mm in diameter and 3 mm in depth) located in the outside wall of the die was used to control and monitor the temperature. Pressure was set at 50 MPa at room temperature and maintained up to the end of the dwell. In each case, pressure was released at the end of the holding time and the cooling rate down to 1000 °C was around 400 °C/min. Some graphite paper, used for the die protection, remaining at the surface of the 3D parts after the SPS step was removed by soft polishing of the samples using abrasive paper. Then, density of the final specimens was determined according to Archimedes' principle and compared to SiC theoretical density.

The structure of the samples was analyzed using Cu K-alpha radiation (λ = 1.5406 Å) across the 2θ range of 20–80° via X-ray powder diffraction (Diffractometer D8 - 2). The phase composition was determined using the Rietveld method from XRD patterns with MAUD, following the strategy developed by Hongchao et al. [26]. Their microstructure was further examined using Scanning Electron Microscopy (LEO435 VP).

To measure the density and porosity of the samples, a high-resolution X-ray microtomography acquisition was performed using the latest"Phoenix X-ray Nanotom"at the

Table 1 Powder bed selective laser processing parameters range used for silicon carbide and surface modified silicon carbide powders

Powder	Laser power (W)	Scanning speed (mm/s)	Hatching distance (µm)	Layer thickness (µm)	Powder compaction (%)	Scanning strategy
SiC and smSiC	35–55	50–1000	18–100	20–40	0–100	Hexagonal

Fédération de Recherche FERMaT FR3089, located at the French Laboratory CIRIMAT UMR CNRS 5085 (Centre Inter-universitaire de Recherche et d'Ingénierie des Matériaux). The image resolution reaches up to 1 micrometer.

Results and discussion

Porosity and relative density

PBSLP-fabricated components prior to SPS treatment

Figures 3 and 4 depict both X-ray microtomography analyses of silicon carbide and surface-modified silicon carbide 3D parts manufactured with the optimized parameters outlined in Table 2. The parameter optimization criteria aimed at producing intact parts with high reproducibility and achieving the highest relative density. In Fig. 3a), silicon carbide 3D part (PBSLP-SiC) sample exhibit 32 ± 1% of porosity. In comparison with other interior volumes of the same sample similar values, have been obtained, specific, 34 ± 1% and 33 ± 1% for the orange and red regions in Fig. 3b). Regarding the porosity of the surface modified

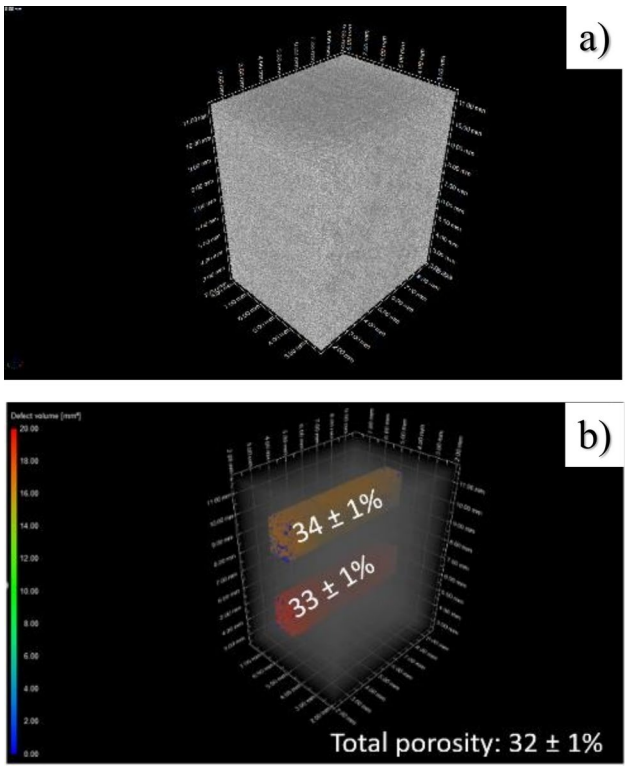

Fig. 3 X-ray micro tomography analysis of silicon carbide 3D parts manufactured using SiC powder (PBSLP-SiC). **a**) Silicon carbide 3D part (PBSLP-SiC) sample exhibit 32 ± 1% of porosity **b**) Interior volumes of the same sample with 34 ± 1% and 33 ± 1% of porosity for the orange and red regions respectively

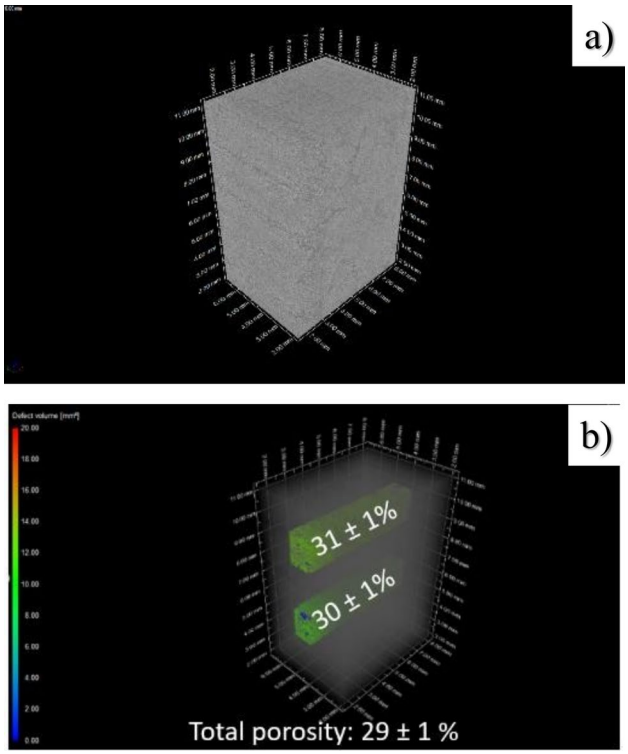

Fig. 4 X-ray micro tomography analysis of silicon carbide 3D parts manufactured using smSiC powder (PBSLP-smSiC). **a**) Silicon carbide 3D part (PBSLP-SiC) sample exhibit 29 ± 1% of porosity **b**) Interior volumes of the same sample with 31 ± 1% and 30 ± 1% of porosity for the top and bot regions respectively

silicon carbide 3D part (PBSLP-smSiC) Fig. 4a), 29 ± 1% of porosity is found. Again, in two different regions inside the sample the porosity is measured, obtaining values of 31 ± 1% and 30 ± 1% Fig. 4b).

Consequently, the relative density measured by the Archimedes method of these various 3D parts reveals differences among the various powders used as starting materials. PBSLP-smSiC samples, prepared with a laser power (P) of 50 W, scanning speed (v) of 500 mm/s, layer thickness of 30 µm, hatching distance of 35 µm, and powder cylinder compaction of 100%, exhibit the highest relative density (71 ± 3%) compared to the PBSLP-SiC samples, prepared with a laser power (P) of 50 W, scanning speed (v) of 250 mm/s, layer thickness of 30 µm, hatching distance of 35 µm, and powder cylinder compaction of 100% (66 ± 6%). Their relative density is approximately 5% higher than that of 3D SiC samples prepared using ungrafted powders, a similar difference found with the X-ray microtomography analysis. Moreover, PBSLP-SiC parts were manufactured using a scanning speed (v) of 250 mm/s instead of 500 mm/s, which results in a decrease in the applied energy density and, therefore, in the temperature reached in the process.

Table 2 Optimized powder bed selective laser processing parameters used for silicon carbide (SiC) and surface modified silicon carbide (smSiC) powders

Powder	Laser Power (W)	Scanning Speed (mm/s)	Hatching distance (µm)	Layer-Thickness (µm)	Powder Compaction (%)	Scanning Strategy
SiC	50	250	35	20	100	Hexagonal
smSiC	50	500	35	20	100	Hexagonal

This shows that only the scanning speed has been significantly increased for smSiC leading to a faster process

The manufacturing of silicon carbide 3D parts via PBSLP, starting from a powder mixture containing α-SiC ($d_{50} = 20$ µm), has been previously documented in literature [25, 27]. Specifically, regarding the SiC powder, using the parameters outlined in Table 2, a change in scanning speed from 250 mm/s to 500 mm/s would lead to a very fragile 3D part with numerous defects and lacking reproducibility. However, for the smSiC powder, employing a scanning speed of 500 mm/s results in a 3D part with higher relative density compared to using SiC powder at 250 mm/s. This observation aligns with findings from previous experiments where SiC and smSiC were densified using Spark Plasma Sintering [22].

Furthermore, the utilization of smSiC powder addresses the challenge of using SiC in direct PBSLP in the absence of other binders or additives due to the lack of a melt phase under normal circumstances. The preceramic precursor creates a reactive interphase between SiC powder grains, facilitating bonding of the ceramic particles without altering the final material phases. Additionally, it renders the debinding process unnecessary, as the polymer is converted into silicon carbide as an integral part of the final material structure.

The mechanism behind the sintering enhancement of grafted powder is as follows: thermal decomposition induced by laser irradiation causes the grafted preceramic precursor to lose H_2, leading to crosslinking and an increase in viscosity until a solid amorphous polymer is obtained. The loss of H_2 and subsequent crosslinking continues until the formation of solid amorphous SiC, followed by polycrystalline SiC [28]. The grafted molecular SiC layer forms a reactive interphase between SiC powder grains, facilitating diffusion and sintering. This results in bonding of the ceramic particles without affecting the final material phases and eliminates the need for the debinding process, as the oligomer is converted into silicon carbide as an integral part of the final material structure.

SPS-treated components from PBSLP manufacturing

On the other hand, X-ray micro tomography analysis of the spark plasma sintered 3D samples of silicon carbide and surface modified silicon are shown in Fig. 5 and in Fig. 6. The details and conditions about the SPS process are given in the previous section. In Fig. 3, silicon carbide SPS 3D

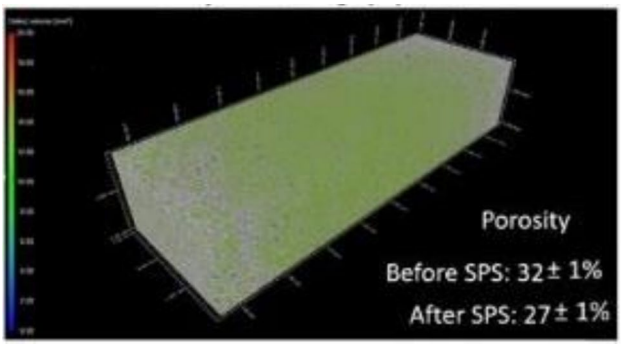

Fig. 5 X-ray micro tomography analysis of silicon carbide 3D parts (PBSLP-SPS-SiC)

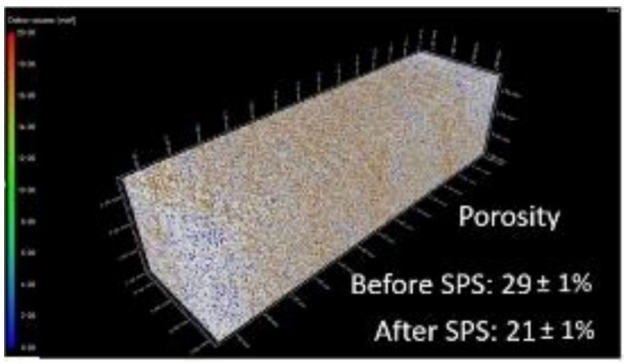

Fig. 6 X-ray micro tomography analysis of silicon carbide 3D parts (PBSLP-SPS-smSiC)

part (PBSLP-SPS-SiC) sample exhibit 26 ± 1 % of porosity. Regarding the porosity of the surface modified silicon carbide SPS 3D part (PBSLP-SPS-smSiC), 21 ± 1 % of porosity is found. The relative density of PBSLP-SPS-smSiC compared to PBSLP-SPS-SiC is approximately 5% higher than that of 3D SiC samples, a very similar value to the PBSLP-smSiC and PBSLP-SiC samples.

The final density of post-treated samples by SPS is 73 ± 1 % and 79 ± 1 %. This indicates that Spark Plasma Sintering improves the final densification of the 3D samples by approximately 10%. Specifically, densification is notably better for smSiC, as the amorphous SiC phase created by the polymer-to-ceramic conversion of the PSE facilitates diffusion and sintering. However, despite efforts, full

densification of SiC samples is not achieved (a summary of the porosity measurements is provided in Table 3). Further optimization of the PBSLP parameters, grafting process, and SiC powder characteristics, such as spherical morphology or multimodal powder size, combined with other well-studied and established techniques like polymer infiltration pyrolysis using the same polycarbosilanes as in this study, could enhance the final densification and yield fully dense SiC bodies by the end of the process.

Table 3 Porosity measurements by X-ray micro tomography analysis of silicon carbide (SiC) and surface modified silicon carbide (smSiC) after PBSLP and SPS

Sample	Porosity (%)
PBSLP-SiC	32 ± 1%
PBSLP-smSiC	29 ± 1%
PBSLP-SPS-SiC	27 ± 1%
PBSLP-SPS-smSiC	21 ± 1%

Microstructural and crystallographic characterization

PBSLP-fabricated components prior to SPS treatment

PBSLP-SiC and PBSLP-smSiC (Fig. 7) parts display comparable grain morphologies. Both samples exhibit porosity, a rough surface, and some microcracks; however, no characteristic patterns attributable to laser scanning, such as needle-like protrusions, are discernible, and no significant differences are evident between them.

The phase composition of PBSLP-SiC and PBSLP-smSiC was investigated using XRD. It was observed that the as-received SiC powder contains only two phases: hexagonal-wurtzite SiC- 6H (also known as α-SiC) and rhombohedral SiC- 15R [26]. However, XRD analysis of PBSLP-SiC and PBSLP-smSiC (Figs. 8 and 9) reveals four different crystal phases: SiC- 6H, SiC- 15R, as originally present in the starting powder, along with residual Silicon and Carbon, respectively. This residual presence of Silicon and Carbon indicates some decomposition during the process, likely caused by the high temperature peaks generated by the scanning strategy. From Table 4, it can be observed that the

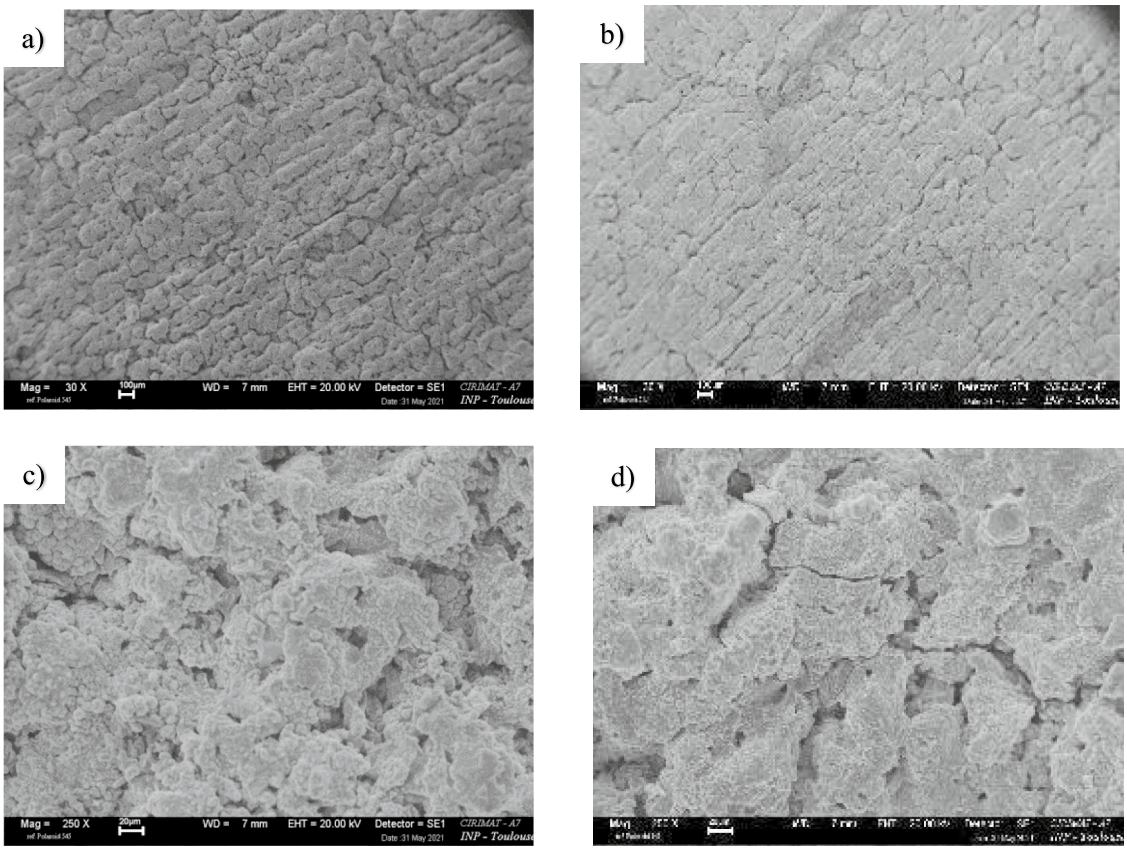

Fig. 7 SEM (Backscatter Detector (CBS)) surface micrographs of the PBSLP-SiC **a**) and **c**) and PBSLP-smSiC **b**) and **d**), with ×30 and ×250 mafnification respectively

proportion of the PBSLP-SiC Silicon phase compared to the PBSLP-smSiC Silicon phase is approximately doubled (15.17% vs. 7.96%), which is consistent with the reduction in energy density when using a scanning speed of 250 mm/s versus 500 mm/s.

These results indicate that the utilization of PSE oligomer as a SiC grafting molecular precursor does not significantly alter the final phase composition of the PBSLP samples, and its conversion to SiC is successfully achieved.

SPS-treated components from PBSLP manufacturing

Regarding PBSLP-SPS-SiC and PBSLP-SPS-smSiC components, they show similar grain morphologies, as shown in

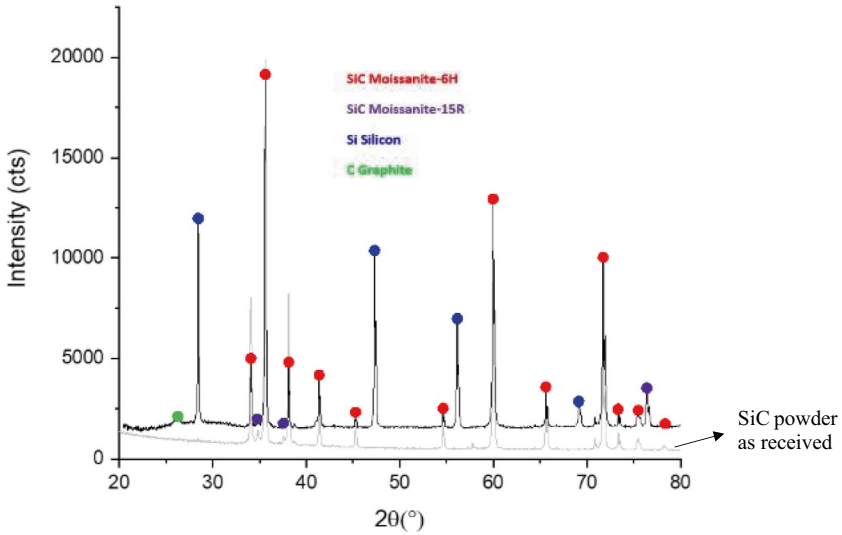

Fig. 8 XRD pattern of PBSLP-SiC compared to the SiC powder (grey)

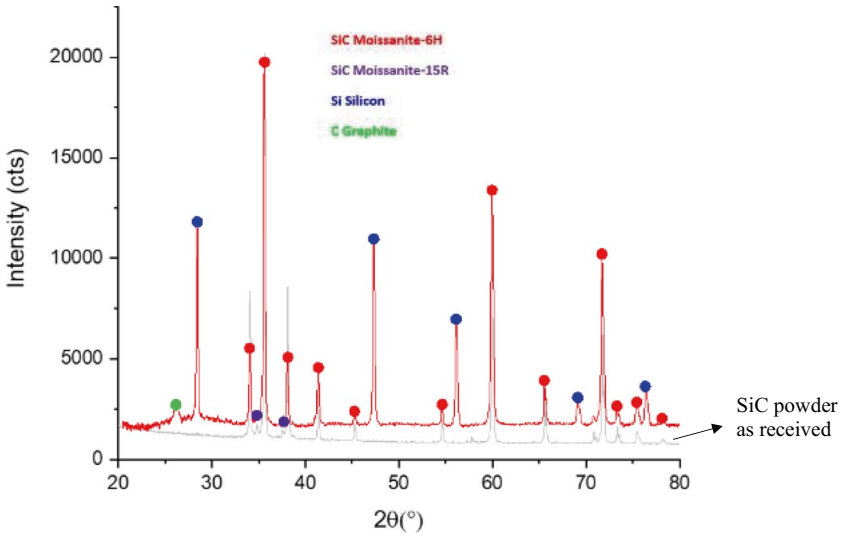

Fig. 9 XRD pattern of a PBSLP-smSiC part (red) compared to the SiC powder (grey). Note that there is no XRD difference between SiC and smSiC powders [22]

Table 4 Phase composition determined by Rietveld method [26] of XRD patterns of SiC powder and SiC 3D part samples as-prepared by PBSLP without SPS post-treatment

Starting powder	Sample name	SiC- 6H	SiC- 15R	Silicon	Carbon	Rwp (%)	Rexp (%)
SiC	PBSLP-SiC	81.93% ± 1.60	1.95% ± 0.01	15.17% ± 1.56	0.95% ± 0.20	10.1	3.1
smSiC	PBSLP-smSiC	90.15% ± 1.93	1.44% ± 0.37	7.96% ± 0.20	0.44% ± 0.01	14.7	3.6

Note: *Rexp* is the expected pattern R-factor, *Rwp* is the weighted pattern R-factor

Figs. 10 and 11. The introduction of Spark Plasma Sintering (SPS) on the 3D samples has influenced the microstructure of these specimens. In the sample without surface modification, there is a noticeable increase in surface porosity. Importantly, both PBSLP-SPS-SiC and PBSLP-SPS-smSiC samples demonstrate a reduction in porosity compared to PBSLP samples, as depicted in Fig. 7, owing to the densification effect of SPS.

On the other hand, the qualitative XRD analysis of PBSLP-SPS-SiC and PBSLP-SPS-smSiC (Fig. 12) reveals three different crystal phases: SiC- 6H, SiC- 15R as originally present in the starting powder, along with residual carbon. The presence of residual carbon can be attributed to contamination by the graphite dies used in the SPS process, and therefore, graphite was not considered in subsequent analysis [22]. In contrast to PBSLP-SiC and PBSLP-smSiC samples, silicon is not detected in these samples. This is because graphite powder, used to fill the empty space between the graphite dies and the sample for SPS densification, reacts with free silicon to form reaction bonded Silicon Carbide (RBSiC). Consequently, this technique not only facilitates the final densification of the 3D parts but also removes free silicon from the sample. However, the formation of Reaction Bonded Silicon Carbide (RBSiC) is primarily observed on the surface of the sample, where the free silicon interacts with the graphite powder used in the process. Since the graphite powder cannot penetrate the pores of the sample, silicon remains present inside the sample. Therefore, the SPS treatment predominantly modifies the composition of the sample at the surface.

Conclusion

An innovative method involving the production of core-shell structured ceramic powders for application in additive manufacturing was employed. Specifically, a SiC preceramic, PSE, was grafted onto the surface of SiC particles in the form of a conformal coverage molecular layer. To assess and compare the efficiency and impact of the surface modification in the manufacturing process, Powder Bed Selective Laser Processing (PBSLP) was conducted to manufacture SiC and surface-modified SiC (smSiC) 3D parts. Silicon carbide and surface-modified silicon carbide parts were manufactured using PBSLP with a laser power (P) of 50 W, scanning speeds (v) of 250 and 500 mm/s, respectively, a layer thickness of 30 µm, hatching distance of 35 µm, and powder cylinder compaction of 100%. The

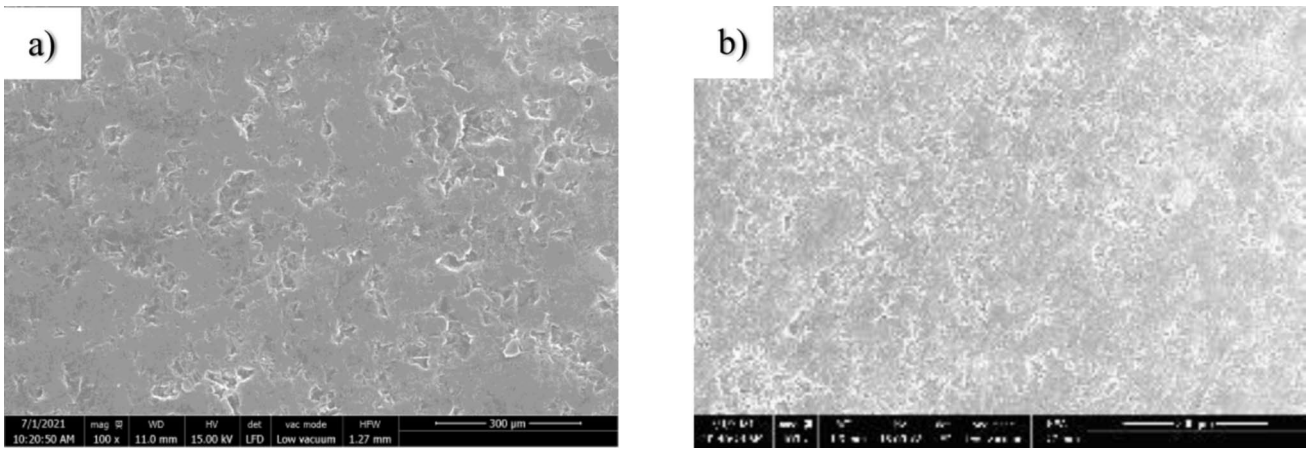

Fig. 10 SEM (Backscatter Detector (CBS)) surface micrographs of the PBSLP-SPS-SiC **a**) and PBSLP- SPS-smSiC **b**) with × 100 magnification

Fig. 11 SEM (Scanning Transmission Electron Detector (STEM)) surface micrographs of the PBSLP-SPS-SiC **a**) and and PBSLP- SPS-smSiC **b**) with × 100 magnification

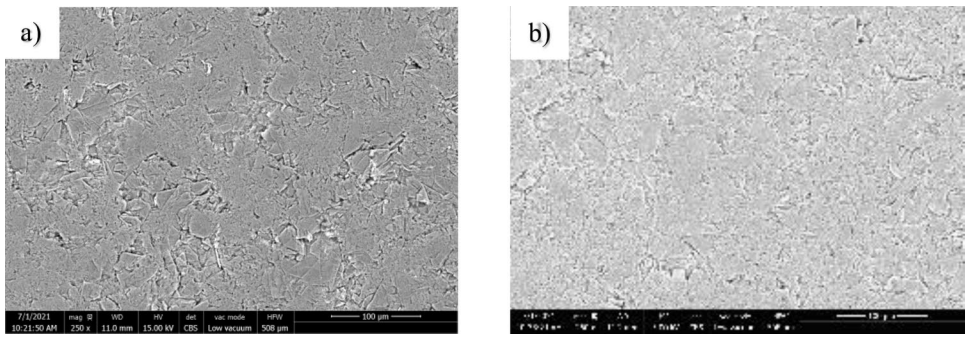

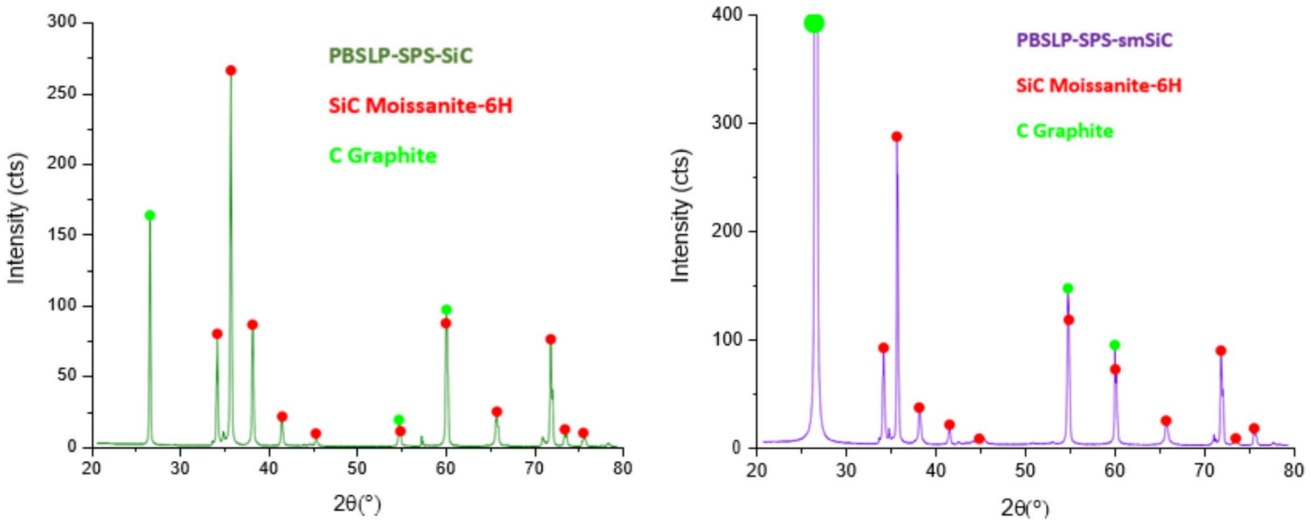

Fig. 12 XRD surface spectra of PBSLP-SPS-SiC (left-green) and XRD surface spectra of PBSLP-SPS-smSiC (right-purple)

final relative density of PBSLP-smSiC was approximately 5% higher than that of 3D SiC samples prepared using ungrafted powders. Moreover, PBSLP-SiC parts were manufactured using a scanning speed (v) of 250 mm/s instead of 500 mm/s, resulting in a decrease in the applied energy density and temperature reached in the process. Consequently, the proportion of the PBSLP-SiC silicon phase compared to the PBSLP-smSiC silicon phase, due to SiC decomposition, doubled (15.17% vs 7.96%). Specifically, a change in scanning speed from 250 mm/s to 500 mm/s would result in a fragile 3D part with many defects using ungrafted powders. However, for the smSiC powder, using a value of 500 mm/s results in a 3D part with higher relative density than using SiC powder and 250 mm/s. This result aligns with observations of reduced sintering initiation in previous experiments where SiC and smSiC were densified using Spark Plasma Sintering (SPS) [22]. Furthermore, the use of smSiC powder addresses the difficulty of using SiC in direct PBSLP in the absence of other binders or additives, due to the lack of a melt phase under normal circumstances. The preceramic precursor creates a reactive interphase between SiC powder grains, resulting in bonding of the ceramic particles without affecting the final material phases and eliminating the need for debinding since the polymer is converted into silicon carbide as an integral part of the final material structure. Therefore, this core-shell structure method presents a new technological impact for the additive manufacturing field, enhancing the sintering behavior of ceramic material in PBSLP. It could be extended to coatings with low melting points to promote liquid phase sintering, increase powder absorptance, or modify viscosity, among other applications. Finally, Spark Plasma Sintering was used to further densify the 3D samples by around 10%. However, in addition to final densification, this technique also removed free silicon from the sample surface, as the graphite powder used for SPS densification reacts with free silicon to form reaction-bonded silicon carbide (RBSiC).

Author contribution All authors contributed to the study conception and design. Material preparation, data collection, and analysis were performed by Alejandro Montón, David Grossin, Francis Maury, and Geoffroy Chevallier. The first draft of the manuscript was written by Alejandro Montón, and all authors commented on previous versions of the manuscript. Claude Estournès and Marc Ferrato provided critical revisions and feedback. All authors read and approved the final manuscript.

Funding Open access funding provided by Institut National Polytechnique de Toulouse. This project, DOC- 3D-printing, has received funding from the European Union's Framework Program for Research and Innovation Horizon 2020 (2014–2020) under the Marie Skłodowska-Curie Grant Agreement No. [764935].

Data availability The datasets generated and/or analyzed during the current study are not publicly available due to their proprietary nature or specific restrictions but are available from the corresponding author, Alejandro Montón (alejandromonton@unizar.es), upon reasonable request. Raw data were generated at CIRIMAT, Université de Toulouse, and MERSEN Boostec. Requests for access to these datasets should include a clear justification for their use in research.

Declarations

Conflicts of interest I am writing to disclose potential conflicts of interest related to the research and publication of "Core–shell powder strategy for Additive Manufacturing of ceramics: Application to Direct Powder Bed Selective Laser Processing of Silicon Carbide", which I am submitting for consideration in Journal of the Australian Ceramic Society.
I confirm that I have disclosed all potential conflicts of interest related to the manuscript and that I have made every effort to ensure that the research and publication of the manuscript are free from any undue influence or bias.

References

1. G. L. Harris and Institution of Electrical Engineers. (eds.): Properties of silicon carbide. INSPEC, the Inst. of Electrical Engineers, London (1995)
2. Ohji, T., Singh, M., Halbig, M. (eds.): Advanced processing and manufacturing technologies for nanostructured and multifunctional materials II: a collection of papers presented at the 39th international conference on advanced ceramics and composites. John Wiley & Sons, Inc., Hoboken (2015). https://doi.org/10.1002/9781119211662
3. Leray, C., et al.: Design and proof of concept of an innovative very high temperature ceramic solar absorber. Abu Dhabi, United Arab Emirates, p. 030032 (2017). https://doi.org/10.1063/1.4984375
4. Bougoin, M., Mallet, F., Lavenac, J., Gerbert Gaillard, A., Ballhause, D., Chaumeil, F.: Full-SiC EUCLID's very large telescope. In: International conference on space optics — ICSO 2018, Chania, Greece, p. 60. (2019). https://doi.org/10.1117/12.2535980
5. Castel, D., Sein, E., Lopez, S., Nakagawa, T., Bougoin, M.: The 3.2m all SiC telescope for SPICA. Amsterdam, Netherlands, p. 84502P (2012). https://doi.org/10.1117/12.926891
6. Grossin, D., et al.: A review of additive manufacturing of ceramics by powder bed selective laser processing (sintering / melting): Calcium phosphate, silicon carbide, zirconia, alumina, and their composites. Open Ceram. **5**, 100073 (2021). https://doi.org/10.1016/j.oceram.2021.100073
7. Veron, F., Lanoue, F., Baco-Carles, V., Kiryukhina, K., Vendier, O., Tailhades, P.: Selective laser powder bed fusion for manufacturing of 3D metal-ceramic multi-materials assemblies. Addit. Manuf. **50**, 102550 (2022). https://doi.org/10.1016/j.addma.2021.102550
8. Meyers, S.: Additive manufacturing of technical ceramics. **178**
9. Magnani, G., Sico, G., Brentari, A., Fabbri, P.: Solid-state pressureless sintering of silicon carbide below 2000°C. J. Eur. Ceram. Soc. **34**(15), 4095–4098 (2014). https://doi.org/10.1016/j.jeurceramsoc.2014.06.006
10. Jin, L., Zhang, K., Xu, T., Zeng, T., Cheng, S.: The fabrication and mechanical properties of SiC/SiC composites prepared by SLS combined with PIP. Ceram. Int. **44**(17), 20992–20999 (2018). https://doi.org/10.1016/j.ceramint.2018.08.134
11. Liu, K., et al.: Laser additive manufacturing and homogeneous densification of complicated shape SiC ceramic parts. Ceram. Int. **44**(17), 21067–21075 (2018). https://doi.org/10.1016/j.ceramint.2018.08.143
12. Song, S., Gao, Z., Lu, B., Bao, C., Zheng, B., Wang, L.: Performance optimization of complicated structural SiC/Si composite ceramics prepared by selective laser sintering. Ceram. Int. S027288421932509X (2019). https://doi.org/10.1016/j.ceramint.2019.09.004
13. Meyers, S., De Leersnijder, L., Vleugels, J., Kruth, J.-P.: Direct laser sintering of reaction bonded silicon carbide with low residual silicon content. J. Eur. Ceram. Soc. **38**(11), 3709–3717 (2018). https://doi.org/10.1016/j.jeurceramsoc.2018.04.055
14. Monton, A., Grossin, D., Maury, F., Abdelmoula, M., Ferrato, M., Küçüktürk, G.: Process parameters investigation for direct powder bed selective laser processing of silicon carbide. Prog. Addit. Manuf. **7** (2022). https://doi.org/10.1007/s40964-022-00305-7
15. Abdelmoula, M., Zarazaga, A.M., Küçüktürk, G., Maury, F., Grossin, D., Ferrato, M.: Scanning strategy investigation for direct powder bed selective laser processing of silicon carbide ceramic. Appl. Sci. **12**(2), 788 (2022). https://doi.org/10.3390/app12020788
16. Guillard, F., Allemand, A., Lulewicz, J.-D., Galy, J.: Densification of SiC by SPS-effects of time, temperature and pressure. J. Eur. Ceram. Soc. **27**(7), 2725–2728 (2007). https://doi.org/10.1016/j.jeurceramsoc.2006.10.005
17. Hayun, S., et al.: Microstructure and mechanical properties of silicon carbide processed by Spark Plasma Sintering (SPS). Ceram. Int. **38**(8), 6335–6340 (2012). https://doi.org/10.1016/j.ceramint.2012.05.003
18. Eqtesadi, S., et al.: Fabricating geometrically-complex B4C ceramic components by robocasting and pressureless spark plasma sintering. Scr. Mater. **145**, 14–18 (2018). https://doi.org/10.1016/j.scriptamat.2017.10.001
19. Manière, C., Nigito, E., Durand, L., Weibel, A., Beynet, Y., Estournès, C.: Spark plasma sintering and complex shapes: The deformed interfaces approach. Powder Technol. **320**, 340–345 (2017). https://doi.org/10.1016/j.powtec.2017.07.048
20. Galusek, D., et al.: Al2O3–SiC composites prepared by infiltration of pre-sintered alumina with a poly(allyl)carbosilane. J. Eur. Ceram. Soc. **31**(1–2), 111–119 (2011). https://doi.org/10.1016/j.jeurceramsoc.2010.09.013
21. Tolochko, N., Mozzharov, S., Laoui, T., Froyen, L.: Selective laser sintering of single- and two-component metal powders. Rapid Prototyp. J. **9**(2), 68–78 (2003). https://doi.org/10.1108/13552540310467077
22. Monton, A., Maury, F., Chevallier, G., Etournes, C., Ferrato, M., Grossin, D.: Densification of surface-modified silicon carbide powder by spark-plasma-sintering. J. Eur. Ceram. Soc. **41**(15), 7543–7551 (2021)
23. Yablokova, G., et al.: Rheological behavior of β-Ti and NiTi powders produced by atomization for SLM production of open porous orthopedic implants. Powder Technol. **283**, 199–209 (2015). https://doi.org/10.1016/j.powtec.2015.05.015
24. Spierings, A.B., Voegtlin, M., Bauer, T., Wegener, K.: Powder flowability characterisation methodology for powder-bed-based metal additive manufacturing. Prog. Addit. Manuf. **1**(1–2), 9–20 (2016). https://doi.org/10.1007/s40964-015-0001-4
25. Abdelmoula, M., Zarazaga, A.M., Küçüktürk, G., Maury, F., Grossin, D., Ferrato, M.: Direct selective laser sintering of silicon carbide: Realizing the full potential through process parameter optimization. Ceramics Int. **49**(20), 32426–32439 (2023). https://doi.org/10.1016/j.ceramint.2023.07.189
26. Hongchao, L., Changlin, K.: Quantitative analysis of SiC polytype distributions by the Rietveld method. J. Mater. Sci. **32**(10), 2661–2664 (1997). https://doi.org/10.1023/A:1018623122324
27. Montón, A., Abdelmoula, M., Küçüktürk, G., Maury, F., Grossin, D., Ferrato, M.: Experimental and numerical study for direct powder bed selective laser processing (sintering/melting) of silicon carbide ceramic. Mater. Res. Express **8**(4), 045603 (2021). https://doi.org/10.1088/2053-1591/abf6fc
28. Boisselier, G., Maury, F., Schuster, F.: SiC coatings grown by liquid injection chemical vapor deposition using single source metal-organic precursors. Surf. Coat. Technol. **215**, 152–160 (2013). https://doi.org/10.1016/j.surfcoat.2012.10.070